

Symmetry breaking in the metal-insulator transition of BaVS₃

T. Inami,¹ K. Ohwada,¹ H. Kimura,² M. Watanabe,² Y. Noda,² H. Nakamura,³ T. Yamasaki,^{3,*} M. Shiga,³ N. Ikeda,⁴ and Y. Murakami^{1,5}

¹Synchrotron Radiation Research Center, Japan Atomic Energy Research Institute, Mikazuki, Hyogo 679-5148, Japan

²Institute of Multidisciplinary Research for Advanced Materials (IMRAM), Tohoku University, Sendai 980-8577, Japan

³Department of Materials Science and Engineering, Kyoto University, Kyoto 606-8501, Japan

⁴Japan Synchrotron Radiation Research Institute, Mikazuki, Hyogo 679-5148, Japan

⁵Department of Physics, Tohoku University, Sendai 980-8578, Japan

(Received 4 March 2002; published 20 August 2002)

It has been believed for a long time that the metal-to-insulator (MI) transition of BaVS₃ is not accompanied by any spatial order of the spin and lattice. We have carried out x-ray-diffraction measurements of BaVS₃ single crystals using a laboratory x-ray source as well as synchrotron radiation, and found that superlattice reflections which double the lattice constant c exist below the transition temperature. The most probable space group at the low-temperature insulator phase contains two inequivalent vanadium sites, and thus a charge disproportionation of the vanadium ions is considered the main cause of the MI transition.

DOI: 10.1103/PhysRevB.66.073108

PACS number(s): 71.30.+h, 61.10.-i, 71.27.+a

A metal-to-insulator (MI) transition is one of the interesting subjects in condensed-matter physics, and is observed in many real materials. According to the dimensionality, band filling, bandwidth, and a certain degree of freedom which shows symmetry breaking, there are a wide variety of transitions,¹ some of which are still controversial in the mechanism, for instance, the Verwey transition in magnetite.^{2,3}

The MI transition in BaVS₃ is one such unresolved issue. In spite of intensive investigations over three decades,⁴⁻¹⁷ the character of the transition is not well understood. One of the largest problems is the driving force of the MI transition. No breaking of symmetry, such as magnetic ordering and structural distortion, which accompanies the MI transition has been reported to date.^{8,9} Hence the order parameter of the transition has been vague, and it is even suggested that the transition is a realization of the pure Mott transition.^{14,15} Another problem is the nature of the insulator phase below the MI transition at $T_{\text{MI}}=70$ K. The magnetic susceptibility shows a Curie-Weiss like behavior above T_{MI} , and decreases steeply below T_{MI} with decreasing temperature.^{5,11,15} This large reduction of the susceptibility is not caused by magnetic ordering. Neutron powder diffraction measurements revealed that no magnetic Bragg reflection appears just below T_{MI} .^{9,16} Instead, Nakamura *et al.* found that long-range incommensurate magnetic order sets in at $T_{\text{X}}=30$ K, well below T_{MI} .¹⁶ The ordered moment was estimated to be $0.5\mu_B/\text{V}$ ion. Therefore, the insulator phase between T_{MI} and T_{X} is a phase which has no magnetic long-range order and suppressed magnetic moments. Nevertheless, the ground state is not a complete singlet and 50% of spins are still magnetic. A model of the MI transition in BaVS₃, therefore, must interpret this complicated magnetic behavior simultaneously. Such a coherent picture of the insulator phase has not been obtained so far.

In this paper, we have performed single-crystal x-ray-diffraction measurements in order to find the hidden order parameter of the MI transition in BaVS₃. Rather surprisingly, it was a structural phase transition, which has long been be-

lieved to be absent. We found superlattice reflections which double the unit cell along the c axis, and confirmed that the intensity of the reflections disappears at T_{MI} . We also carried out a preliminary check of the space group using synchrotron radiation. Based on the obtained results, the origin of the MI transition is discussed.

BaVS₃ crystallizes into a hexagonal structure (space group $P6_3/mmc$, $a=6.719$ Å, and $c=5.619$ Å) at room temperature, which is characterized by VS₃ chains running along the c axis [Fig. 1(a)]. A structural phase transition takes place at $T_S=240$ K, and the crystal system becomes orthorhombic. Since the transition is of second-order type, the space group below T_S is considered $Cmcm$ or its subgroups.^{9,8} We use the space group $Cmcm$ in this paper, because the suggested space group $Cmc2_1$ is incompatible with our observation. As already mentioned, BaVS₃ undergoes a MI transition at $T_{\text{MI}}=70$ K from the high-temperature metallic phase to the low-temperature insulator phase, which is followed by a magnetic phase transition with a propagation vector $Q=(0.226, 0.226, 0)$ in a hexagonal setting at $T_{\text{X}}=30$ K [Fig. 1(b)].

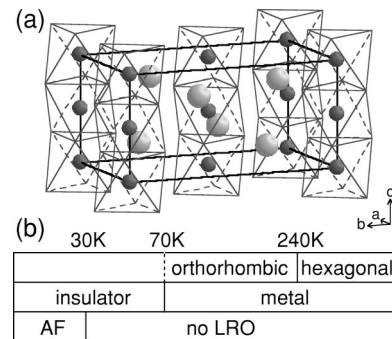


FIG. 1. (a) Crystal structure of BaVS₃ at the orthorhombic phase ($Cmcm$). Large and small shaded spheres show barium and vanadium ions, respectively. The sulfur ions reside at the vertices of the octahedra. (b) Structural, transport, and magnetic properties of BaVS₃ as a function of temperature. AF is the antiferromagnetically ordered phase.

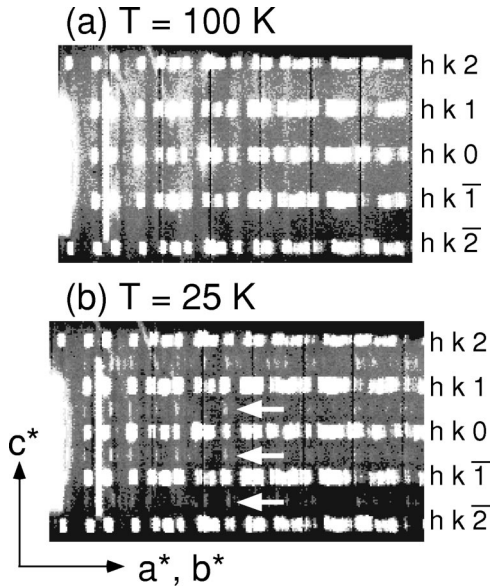


FIG. 2. Oscillation photographs of BaVS_3 . (a) At 100 K (above T_{MI}). The white points are fundamental Bragg reflections hkl , and are classified by l from bottom ($l = -2$) to top ($l = 2$). (b) At 25 K (below T_{MI}). Superlattice reflections are observed on $l = n + \frac{1}{2}$ lines. Three superlattice points are shown by arrows.

Single crystals in needlelike shapes were synthesized by a tellurium flux method, and then were annealed in the presence of sulfur vapor in order to compensate for deficient sulfur.¹⁸ The x-ray-diffraction measurements were carried out using a two-axis diffractometer at IMRAM, Tohoku University.¹⁹ $\text{Mo } K\alpha$ radiations from a rotating anode (50 kV, 60 mA) were monochromatized by a pyrolytic graphite 002 crystal. The scattered x rays were detected by an image plate as well as a sodium-iodine scintillation detector. A single crystal, the dimensions of which are $\phi 0.2 \times 3 \text{ mm}^2$, was mounted on the cold finger of a closed-cycle He refrigerator. Due to the large sample size, the sample was a multidomain below the structural transition at T_S . The sample mosaic spread also became broad from 0.13° (300 K) to 1.5° (25 K).

We also performed synchrotron x-ray-diffraction measurements at beamline BL02B1 of SPring-8.²⁰ Synchrotron radiations were monochromatized by a Si 311 double-crystal monochromator, and higher harmonics were eliminated by the use of mirrors. The x-ray energy was 30 keV. A small single crystal was mounted on the cold finger of a closed-cycle He refrigerator on a four-circle diffractometer. Because of the small sample size ($100 \times 100 \times 150 \mu\text{m}^3$), the sample was single-domain below T_S . The sample mosaic was about 0.16° at low temperatures. In addition, the transmission of x-rays at 30 keV through BaVS_3 of 100 μm thick is about 75%, and hence the absorption correction to the diffracted intensity is not very significant for this small crystal.

We first took oscillation photographs at 100 K (above T_{MI}) and at 25 K (below T_{MI}) using an image plate. The c axis of the sample was vertical to the scattering plane, and the sample was rotated about the c axis by 30° . The results are shown in Fig. 2. The vertical direction of the photograph

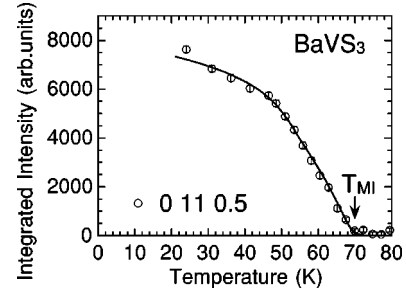


FIG. 3. Integrated intensity of the superlattice reflection $0\ 11\ \frac{1}{2}$ as a function of temperature. The intensity decreases with increasing temperature, and vanishes just at the transition temperature T_{MI} ($=70 \text{ K}$).

corresponds to the crystalline c^* axis, while the horizontal direction is the superposition of the a^*-b^* plane. Thus Bragg reflections hkl appear as horizontal lines with different values of l in the photographs. Above T_{MI} , no significant intensity is observed other than the fundamental Bragg lines. In contrast, well below T_{MI} , weak superlattice reflections are clearly observed just midway between the Bragg lines, indicating a structural phase transition which doubles the c axis exists below T_{MI} . We then measured Weissenberg photographs of the $(h, k, 0)$, $(h, k, \frac{1}{2})$, and $(h, k, 1)$ planes at 25 K. In the $(h, k, 0)$ and $(h, k, 1)$ planes, only fundamental reflections were observed at $h+k=2n$. No additional peak was found. On the other hand, in the $(h, k, \frac{1}{2})$ plane, superlattice reflections were observed at $h+k=2n+1$. Accordingly, the reflection condition is $h+k+2l=2n$ for hkl , and thus it was found that the superlattice is an I lattice (body-centered lattice). In the $(h, k, \frac{1}{2})$ plane, superlattice reflections are intense around the b^* axis, while no peak is found around the a^* axis.

In order to show that the observed structural distortion is associated with the MI transition, the intensity of a superlattice reflection was measured as a function of temperature using a scintillation detector. As shown in Fig. 3, the integrated intensity at $(0, 11, \frac{1}{2})$ decreases smoothly with increasing temperature, and vanishes just at T_{MI} , as a characteristic of a second-order phase transition. The result definitely illustrates that the structural distortion (or what directly couples to the structural distortion) is the primary order parameter of the MI transition.

The space group gives crucial information about the type of structural phase transition which takes place at T_{MI} . Synchrotron radiation experiments were carried out for an estimation of the space group below T_{MI} . We first confirmed the reflection condition. We measured reflections on the $(0, 0, l)$, $(0, k, \frac{1}{2})$, $(h, 0, \frac{1}{2})$ and $(h, 0, 1)$ lines at 30 K, and a weak but finite intensity of superlattice reflections at $(h, 0, \frac{1}{2})$ was observed. The total reflection conditions were as follows; for the superlattice ($c' = 2c$), hkl : $h+k+l=2n$, $hk0$: $h+k=2n$, $h0l$: $h+l=2n$, $0kl$: $k+l=2n$, $h00$: $h=2n$, $0k0$: $k=2n$, and $00l$: $l=2n$. This shows that the superlattice is an I lattice without any glide plane.

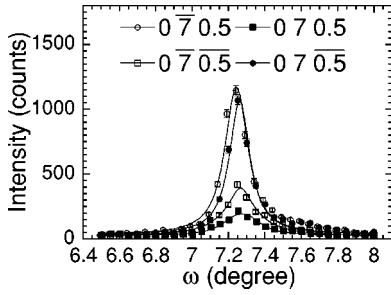


FIG. 4. Rocking curves of four symmetric superlattice reflections in the b^*-c^* plane. The asymmetry of superlattice reflections in intensity suggests that the mirror planes perpendicular to the b and c axes and the twofold axes parallel to the b and c axes are missing.

We then confirmed the Laue symmetry of the lattice. Four superlattice reflections at $(0, \pm 7, \pm 0.5)$ are shown in Fig. 4. Obviously the $I(\vec{Q})$ s (the diffracted intensity at a momentum transfer \vec{Q}) are not all identical, although the momentum transfers are symmetric. Since the condition that $I(\vec{Q}) = I(-\vec{Q})$ (the so-called Friedel pair) is fulfilled, that is $I(0, 7, 0.5) \cong I(0, \bar{7}, 0.5)$ and $I(0, \bar{7}, 0.5) \cong I(0, 7, \bar{0.5})$, the effect of absorption is considered rather small in these data. Inequality in the diffracted intensities therefore indicates the lack of mirror planes perpendicular to the b and c axes and the twofold axes parallel to the b and c axes. We could not obtain convincing data for superlattice reflections including the a^* axis, because of the weak intensity. Although the observed lattice constant α was nearly 90° , the data shown in Fig. 4 imply that the crystal structure below T_{MI} is a monoclinic lattice of the unique a axis.

Combining the results for the reflection conditions and the Laue symmetry, possible space groups are $I211$, $Im11$, and $I2/m11$. Since it seems that the MI transition is of second order, the space group below T_{MI} is a subgroup of the space group above T_{MI} ($Cmcm$). Under this restriction, relations between $Cmcm$ and the possible low-temperature space groups are summarized in Table I.²¹

It is likely that the overall pattern of superlattice reflections in a monoclinic lattice should be reminiscent of that in its supergroup. In this sense, the space group $I211$ is not plausible. The space group $I2/c11$ (the supergroup of $I211$) has a reflection condition $k, l = 2n$ for $0kl$, and hence there is no superlattice reflection at $(0, k, \frac{1}{2})$. However, the observed pattern of superlattice reflections in the $(h, k, \frac{1}{2})$ plane is weak around the a^* axis and strong around the b^* axis. On the other hand, the reflection conditions of $Im2m$ are the same as the observed ones. In addition, the relatively strong intensity of the superlattice reflections suggests that the intensity mainly arises from the displacement of the heavy Ba

TABLE I. Group-subgroup chains for subgroups of $Cmcm$ which satisfy the reflection condition and the Laue symmetry.

(i)	$Cmcm \rightarrow C2/m11 \rightarrow I2/c11 \rightarrow I211$
(ii)	$Cmcm \rightarrow Cm2m \rightarrow Im2m \rightarrow Im11$

ions. The observed weak intensity of superlattice reflections around the a^* axis indicates that the displacement of the Ba ions parallel to the a axis is small. In the space group $Im2m$, the Ba ions are at $2a(0, y, 0)$, $2b(0, y, \frac{1}{2})$, and $4c(0, y, z$ and $0, y, \bar{z})$ sites, and actually there is no displacement from highly symmetric positions along the a axis. Accordingly, the best candidate for the space group below T_{MI} is $Im11$. We also think that the space group $Im2m$ (the supergroup of $Im11$) already contains major features of the transition, because superlattice reflections appear at this space group. In the following discussion about the order parameter of the MI transition, we postulate that the space group below T_{MI} is $Im2m$.

A notable difference between the space groups $Cmcm$ and $Im2m$ is the number of vanadium sites. All vanadium ions occupy the equivalent $4a$ site in $Cmcm$, whereas in $Im2m$ the vanadium ions are divided into two crystallographically independent $4c$ sites (we refer to them as V_A and V_B) and pairs of the same kind of the vanadium ions align along the c axis in an alternative manner - $V_A^- V_A^- V_B^- V_B^- V_A^- V_A^- V_B^- V_B^-$. It is therefore likely that a charge disproportionation (CD) of the vanadium ions is the major driving force of the MI transition in $BaVS_3$. The CD is probably partial, i.e., $2V^{4+} \rightarrow V^{4+\delta} + V^{4-\delta}$, $\delta \approx 0$. If $\delta \approx 1$, a large modulation of the spin density along the c axis is expected, because V^{5+} ions have no magnetic moment. However, such a modulation was not observed in neutron diffraction experiments.¹⁶

One might regard this charge (and structural) modulation along the c axis as being caused by a Peierls-type transition due to the chain-like structure of $BaVS_3$. However, the electronic conductivity of $BaVS_3$ is not highly anisotropic and rather three dimensional.¹⁵ A band structure calculated by Mattheiss also exhibits only weak anisotropic features.²² The MI transition in $BaVS_3$ may not stem from a Peierls-type instability.

The huge reduction of the susceptibility at T_{MI} is still an open question. In the space group $Im2m$, the vanadium ions make pairs along the c axis. The atomic coordinates of the vanadium ions are $(0, y, z)$ and $(0, y, \bar{z})$, and thus the vanadium ions are no longer equidistant along the vanadium chain (the c axis). We consider $V_A^- V_A$ and $V_B^- V_B$ pairings here. Supposing that the coupling between V_A spins is antiferromagnetic, the suppression of the magnetic susceptibility at the MI transition can be ascribed to the formation of singlet pairs. On the other hand, the coupling between the V_B spins must be ferromagnetic (otherwise the ground state becomes a singlet) and the surviving V_B spins cause a magnetic long-range order at 30 K. However, this scenario also results in a large modulation of the spin density along the c axis and fails to explain the neutron-diffraction results.¹⁶ Finally, we mention the structure between the chains. In the $z=0$ and $\frac{1}{2}$ planes, the V_A and V_B ions cause stripes, which show an alternate alignment along the b axis, and an expected positional modulation of the Ba ions caused by this stripe order is consistent with the observed intense superlattice reflections around the b^* axis.

In summary, an x-ray-diffraction study of single-crystal $BaVS_3$ has been made, and a structural phase transition

which accompanies the MI transition was found. The symmetry consideration suggests that a pronounced feature of the insulator phase is two inequivalent vanadium sites, and from this result we propose a charge disproportionation of the vanadium ions as a possible origin of the MI transition. Although the magnetic properties of the low-temperature insulator phase are not fully accounted for as yet, a solid basis for further experimental and theoretical investigations on this MI transition is established.

This work was partially supported by Grants-in-Aid for Scientific Research of the Japan Society for the Promotion of Science (11440107, 12640345) and a Grant-in-Aid on priority area "Novel Quantum Phenomena in Transition Metal Oxides" from the Ministry of Education, Science, Sports and Culture (12046243). The synchrotron radiation experiments were performed at the SPring-8 with the approval of the Japan Synchrotron Radiation Research Institute (JASRI) (Proposal No. 2001A0046ND-np).

*Present address: Graduate School of Human and Environmental Studies, Kyoto University, Kyoto 606-8501, Japan

¹M. Imada, A. Fujimori, and Y. Tokura, *Rev. Mod. Phys.* **70**, 1039 (1998).

²J. García *et al.*, *Phys. Rev. B* **63**, 054110 (2001).

³J.P. Wright, J.P. Attfield, and P.G. Radaelli, *Phys. Rev. Lett.* **87**, 266401 (2001).

⁴R.A. Gardner, M. Vlasse, and A. Wold, *Acta Crystallogr., Sect. B: Struct. Crystallogr. Cryst. Chem.* **25**, 781 (1969).

⁵M. Takano *et al.*, *J. Chem. Phys.* **43**, 1101 (1977).

⁶A. Heidemann and M. Takano, *Phys. Status Solidi B* **100**, 343 (1980).

⁷H. Nishihara and M. Takano, *J. Phys. Soc. Jpn.* **50**, 426 (1981).

⁸F. Sayetat, M. Ghedira, J. Chenavas, and M. Marezio, *J. Phys. C* **15**, 1627 (1982).

⁹M. Ghedira, M. Anne, J. Chenavas, M. Marezio, and F. Sayetat, *J. Phys. C* **19**, 6489 (1986).

¹⁰M. Nakamura *et al.*, *Phys. Rev. B* **49**, 16 191 (1994).

¹¹T. Graf, D. Mandrus, J.M. Lawrence, J.D. Thompson, and P.C. Canfield, *Phys. Rev. B* **51**, 2037 (1995).

¹²H. Nakamura, H. Imai, and M. Shiga, *Phys. Rev. Lett.* **79**, 3779 (1997).

¹³C.H. Booth, E. Figueroa, J.M. Lawrence, M.F. Hundley, and J.D. Thompson, *Phys. Rev. B* **60**, 14 852 (1999).

¹⁴L. Forró *et al.*, *Phys. Rev. Lett.* **85**, 1938 (2000).

¹⁵G. Mihály *et al.*, *Phys. Rev. B* **61**, R7831 (2000).

¹⁶H. Nakamura *et al.*, *J. Phys. Soc. Jpn.* **69**, 2763 (2000).

¹⁷I. Kézsmárki, S. Csonka, H. Berger, L. Forró, P. Fazekas, and G. Mihály, *Phys. Rev. B* **63**, 081106 (2001).

¹⁸H. Kuriyaki *et al.*, *Synth. Met.* **71**, 2049 (1995).

¹⁹Y. Kuroiwa, I. Tamura, F. Ohe, H. Jidaisho, K. Akiyama, and Y. Noda, *J. Appl. Crystallogr.* **25**, 341 (1995).

²⁰Y. Noda *et al.*, *J. Synchrotron Radiat.* **5**, 485 (1998).

²¹*International Tables for Crystallography*, edited by T. Hahn (Reidel, Dordrecht, 1983) Vol A.

²²L.F. Mattheiss, *Solid State Commun.* **93**, 791 (1995).